Lymphocytes From Patients With Type 1 Diabetes Display a Distinct Profile of Chromatin Histone H3 Lysine 9 Dimethylation
An Epigenetic Study in Diabetes

Feng Miao,[1] David D. Smith,[2] Lingxiao Zhang,[1] Andrew Min,[1] Wei Feng,[1] and Rama Natarajan[1]

OBJECTIVE—The complexity of interactions between genes and the environment is a major challenge for type 1 diabetes studies. Nuclear chromatin is the interface between genetics and environment and the principal carrier of epigenetic information. Because histone tail modifications in chromatin are linked to gene transcription, we hypothesized that histone methylation patterns in cells from type 1 diabetic patients can provide novel epigenetic insights into type 1 diabetes and its complications.

RESEARCH DESIGN AND METHODS—We used chromatin immunoprecipitation (ChIP) linked to microarray (ChIP-chip) approach to compare genome-wide histone H3 lysine 9 dimethylation (H3K9me2) patterns in blood lymphocytes and monocytes from type 1 diabetic patients versus healthy control subjects. Bioinformatics evaluation of methylated candidates was performed by Ingenuity Pathway Analysis (IPA) tools.

RESULTS—A subset of genes in the type 1 diabetic cohort showed significant increase in H3K9me2 in lymphocytes but not in monocytes. *CLTA4*, a type 1 diabetes susceptibility gene, was one of the candidates displaying increased promoter H3K9me2 in type 1 diabetes. IPA identified two high-scoring networks that encompassed genes showing altered H3K9me2. Many of them were associated with autoimmune and inflammation-related pathways, such as transforming growth factor-β, nuclear factor-κB, p38 mitogen-activated protein kinase, toll-like receptor, and interleukin-6. IPA also revealed biological relationships between these networks and known type 1 diabetes candidate genes.

CONCLUSIONS—The concerted and synergistic alteration of histone methylation within the identified network in lymphocytes might have an effect on the etiology of type 1 diabetes and its complications. These studies provide evidence of a novel association between type 1 diabetes and altered histone methylation of key genes that are components of type 1 diabetes–related biological pathways and also a new understanding of the pathology of type 1 diabetes. *Diabetes* **57:3189–3198, 2008**

Type 1 diabetes is an autoimmune disease resulting from complex interactions between genetic and environmental factors. It is characterized by T-cell–mediated destruction of the insulin-producing β-cells of pancreatic islets. More than 30 genome loci have been linked to type 1 diabetes susceptibility through genome linkage analysis (1). Although numerous genetic studies, including the recent genome-wide association study (2), have provided a wealth of knowledge about genetic factors associated with type 1 diabetes, the underlying mechanisms and pathways causing type 1 diabetes remain only partly understood (3). Genetic approaches in general cannot fully take into consideration the interplay between genes and the environment in type 1 diabetes. As such, a study of the role of epigenetics in type 1 diabetes can provide valuable new insights.

Nuclear chromatin is a crucial interface between the effects of genetics and environment and the principal carrier of epigenetic information. The chromatin is constantly affected by environmental stimuli, such as diet, chemicals, and pathogens (4). The basic repeat unit of chromatin is the nucleosome, which consists of two copies each of histones H2A, H2B, H3, and H4 and is wrapped by 147 bp DNA (5). Notably, the posttranslational modifications (PTMs) of histone tails in chromatin have been linked to gene transcription (6,7). The "histone code" hypothesis has changed our view of histones as being mainly a DNA scaffold to a key regulatory layer of gene transcription. By interacting with various chromatin factors and regulatory proteins, histone PTMs can alter the architecture of chromatin and gene expression. Abnormal alterations in these interactions that cause relatively stable epigenetic changes at the chromatin level could lead to dysregulated gene transcription, metabolic memory (8–10), and disease progression. We sought to obtain evidence for this by genome-wide mapping of a key chromatin mark, histone H3 dimethylated at lysine 9 (H3K9me2). This mark, broadly spread within the human genome, is generally associated with gene repression and could either be a repressive mark in euchromatin or a hallmark feature of heterochromatin (11–13).

Chromatin immunoprecipitation (ChIP) coupled to DNA microarray analysis, or ChIP-chip, is a widely used approach for acquiring genome-wide information on histone modifications (14–18). We recently implemented this approach to profile and compare the variations in histone H3K4me2 and H3K9me2 in human gene coding and CpG island regions in THP-1 monocytes cultured in normal and

high glucose (19). We observed that the treatment of monocytes with high glucose to mimic diabetic conditions could lead to key variations in H3K9me2 in the promoter and coding regions of several genes, including those relevant to the pathogenesis of diabetes (19). In the present study, we have used three types of microarrays (CpG, cDNA, and promoter tiling arrays) to compare, for the first time to our knowledge, the H3K9me2 profiles of blood lymphocytes and monocytes obtained directly from type 1 diabetic patients versus healthy control subjects. Analyses of the data revealed a group of genes showing a striking alteration in histone H3K9me2 in the lymphocytes of the type 1 diabetic patients relative to healthy control subjects and their strong associations to type 1 diabetes. In addition, by applying the bioinformatics software Ingenuity Pathway Application (IPA), we uncovered key biological relationships among a subset of genes in the differentially methylated group and their relevance to type 1 diabetes.

RESEARCH DESIGN AND METHODS

Human subject enrollment. An informed consent form was obtained from all volunteers before blood samples were drawn with an approved institutional review board protocol at the City of Hope General Clinical Research Center. We prospectively enrolled 16 volunteers into two groups, the first with 9 patients having a diagnosis of type 1 diabetes for >10 years (median 16 years, range 11–52 years), and the second with 7 healthy volunteers. No history of autoimmunity was reported in healthy control subjects, and their autoantibody status was not tested. Patient demographics are shown in Fig. 1C. There were no statistically significant differences between age or sex proportion in the two comparison groups. Blood lymphocytes and monocytes from these volunteers were separated using the Ficoll method as described previously (20) (details provided in supplemental methods available in an online appendix at http://dx.doi.org/10.2337/db08-0645). The purity was ~85% for both monocyte and lymphocyte fractions. Both cell types were used for ChIP experiments.
DNA microarrays. Human 12K cDNA arrays were from the University of Pennsylvania Functional Genomics Core, and human 12K CpG island arrays (containing 12,192 CpG island clones) were from the Universal Health Network Microarray Center (Toronto) as described previously (19,20). Human promoter tiling arrays containing 24,659 well-characterized RefSeq genes were from Roche Nimblegen.
ChIP and ChIP-chip experiments. Conventional ChIPs and the ChIP-chips were performed as described previously (15). Purified blood monocytes and lymphocytes from type 1 diabetic and healthy control subjects were cross-linked and sonicated to shear DNA. One-tenth of total lysate was used for "no-antibody" control. ChIPs were then performed with the anti–dimethyl-histone H3K9 (Upstate Biotechnology). Details are provided in the supplemental methods in the online appendix.

Human promoter tiling arrays were hybridized, and the data were extracted according to standard operating procedures by NimbleGen Systems. Signal-Map software from NimbleGen Systems was used to visualize the array peaks.
Microarray data collection and statistical analysis of microarray data. Microarray images were scanned with a GenePix 4000B scanner and quantified with GenePix Pro version 4.1.1.31 (Molecular Devices, Sunnyvale, CA). We then imported the raw data from GenePix into R/Bioconductor statistical software (21–24). We powered our study to detect large differences in up- or downregulation across all probes. Based on our previous results (20), we found that the SD for lymphocyte ChIP-chip data in this population was ~0.5 on the log2 scale in the healthy volunteers. Assuming a two-sided test at 0.05 and 80% power, approximately eight subjects in each group allowed us to detect log2 effect sizes of 0.75 or greater (fold change of 1.68 or greater). We excluded one normal subject after ChIP-chip because of technical problems with the hybridization seen in Fig. 1B. We also excluded one type 1 diabetic patient's ChIP-chip data because of a history of prostate cancer. Full details of the statistical analysis of microarray data are provided in the supplemental methods in the online appendix.
Real-time quantitative PCRs. Real-time quantitative PCRs were performed as described previously (19). Student's t tests were used for statistical analyses of the data. Sequences of primers are provided in the supplemental methods in the online appendix.
IPA. Core bioinformatics analyses were performed by the IPA (www.ingenuity.com). IPA is a knowledge repository of networks and biological relationships that have been systematically encoded into ontology based on >200,000 original peer-reviewed articles. Details and technical requirements are available in the IPA Web site (25) and in the supplemental methods in the online appendix.

RESULTS

ChIP-chip profiling of histone methylation in blood cells of type 1 diabetic patients and healthy control subjects. Fig. 1A demonstrates the experimental design for this study. Primary lymphocytes and monocytes were isolated from the peripheral blood of two cohorts, type 1 diabetic patients and healthy control subjects, and used for ChIP assays with anti–dimethyl-histone H3K9. Antibody-enriched DNA samples and no-antibody controls were prepared from monocytes and lymphocytes of each volunteer separately. They were then analyzed by ChIP-chip by hybridizing to three microarray platforms, i.e., 12K human cDNA, 12K CpG island, and promoter tiling arrays.

Because type 1 diabetes is an autoimmune and T-cell–dysregulated disease, we sought to determine whether lymphocytes isolated from type 1 diabetic patients exhibit any variations in histone lysine methylation relative to healthy control subjects. We first profiled H3K9me2 in lymphocytes from a group of type 1 diabetic patients and healthy control subjects by ChIP-chip using human 12K cDNA arrays. The hierarchical clustering analysis (Fig. 1B) shows that this methylation mark has similar distribution patterns in gene coding regions in lymphocytes among all of the individuals of both groups despite age or sex as recently noted (20). Interestingly, however, there is a clearly visible and consistent cluster or subset of genes showing increased H3K9me2 in lymphocytes of type 1 diabetic patients relative to healthy control subjects (Fig. 1B, see enlarged region for clarity). These data demonstrate 1) that histone methylation distribution patterns in specific human cells are relatively stable in multiple individuals despite age or sex; and 2) that a group of genes consistently displays aberrant H3K9me2 patterns in lymphocytes of type 1 diabetic patients. These data support our ChIP-chip approach to detect variations in histone methylation patterns between two separate groups to provide meaningful and disease-associated information.
Alterations of H3K9me2 between type 1 diabetic patients and healthy control groups are visible in lymphocytes but not in monocytes. To identify specific genes whose histone H3K9me2 status showed differences between type 1 diabetic patients and healthy control subjects, we developed a two-step analysis procedure to retrieve the genome-wide methylation alterations (details in the supplemental methods in the online appendix). We assumed that the histone methylation pattern is "normal" in healthy control subjects and defined "alteration" as the differences in histone methylation when type 1 diabetic patients were compared with healthy control subjects. In the ChIP-chips with 12K cDNA arrays, significance analysis of microarrays (SAM) (26) showed distinct variations in H3K9me2 between the two cohorts in their lymphocyte populations (Fig. 2A, a)but not in monocytes (Fig. 2A, b). Red points in Fig. 2A, a represent probes in which type 1 diabetic patients had higher methylation than healthy control subjects (594 probes were reported within false discovery rate [FDR] < 1%); green points represent probes in which healthy control subjects had higher methylation than type 1 diabetic patients (174 probes were reported within FDR <1%). In addition, the variations in H3K9me2 were type 1 diabetes specific because no statistically
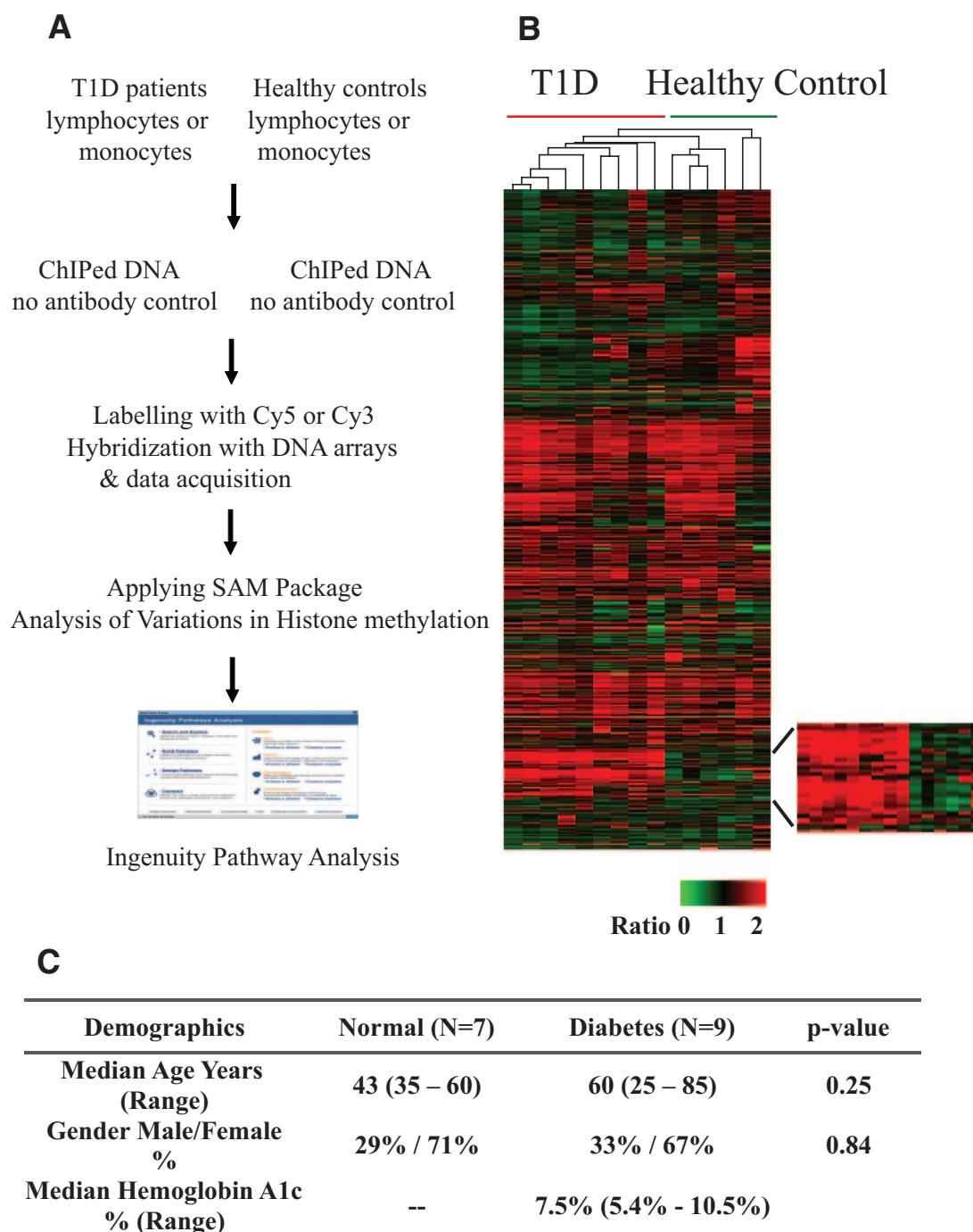
A

T1D patients
lymphocytes or
monocytes

Healthy controls
lymphocytes or
monocytes

↓

ChIPed DNA
no antibody control

ChIPed DNA
no antibody control

↓

Labelling with Cy5 or Cy3
Hybridization with DNA arrays
& data acquisition

↓

Applying SAM Package
Analysis of Variations in Histone methylation

↓

Ingenuity Pathway Analysis

B

T1D   Healthy Control

Ratio   0   1   2

C

Demographics	Normal (N=7)	Diabetes (N=9)	p-value
Median Age Years (Range)	43 (35 – 60)	60 (25 – 85)	0.25
Gender Male/Female %	29% / 71%	33% / 67%	0.84
Median Hemoglobin A1c % (Range)	--	7.5% (5.4% - 10.5%)	

FIG. 1. Profiling histone lysine methylation in blood cells from type 1 diabetic (T1D) patients versus healthy control subjects. *A*: The overall experimental design. *B*: Hierarchically clustered histone H3K9me2 profiles of lymphocyte samples from patients with type 1 diabetes and healthy control subjects (columns) and 10,053 probes (rows). Of the total 12,055 probes in the 12K cDNA array, 2,002 probe signal intensities were below the threshold limit of detection, and this yielded 10,053 probes. The region at the *bottom* showing clear differences in a subset of genes in type 1 diabetes is depicted in the enlarged section on the *right*. *C*: Demographics for the type 1 diabetic patients and healthy control subjects. SAM, significance analysis of microarrays. (Please see http://dx.doi.org/10.2337/db08-0645 for a high-quality digital representation of this figure.)

significant variations were observed when individuals were grouped based on age or sex (Fig. 2*A*, *c* and *d*). Then, based on our requirement of altered histone modification status and a twofold difference criteria (19), 193 of the 594 probes were increased by at least twofold, and these were identified as "increased" H3K9me2 genes in the 12K cDNA array. These are represented in the heatmap in Fig. 2*A*, *right panel*, showing relative methylation levels between type 1 diabetic patients and healthy control subjects. Specifically, genes meeting our criteria are unmethylated in healthy control subjects but have shifted to a methylated state in type 1 diabetic patients. Detailed gene information is listed in supplementary Table S1 (available in the online appendix). Unexpectedly, we could not identify the "decreased" H3K9me2 candidate genes in the type 1 diabetic group because all of 174 probes from Fig. 2*A* showing a decrease in H3K9me2 failed to meet our requirements of altered histone modification status and a twofold difference criteria. Thus, all 174 probes are in an unmethylated state in both cohorts.
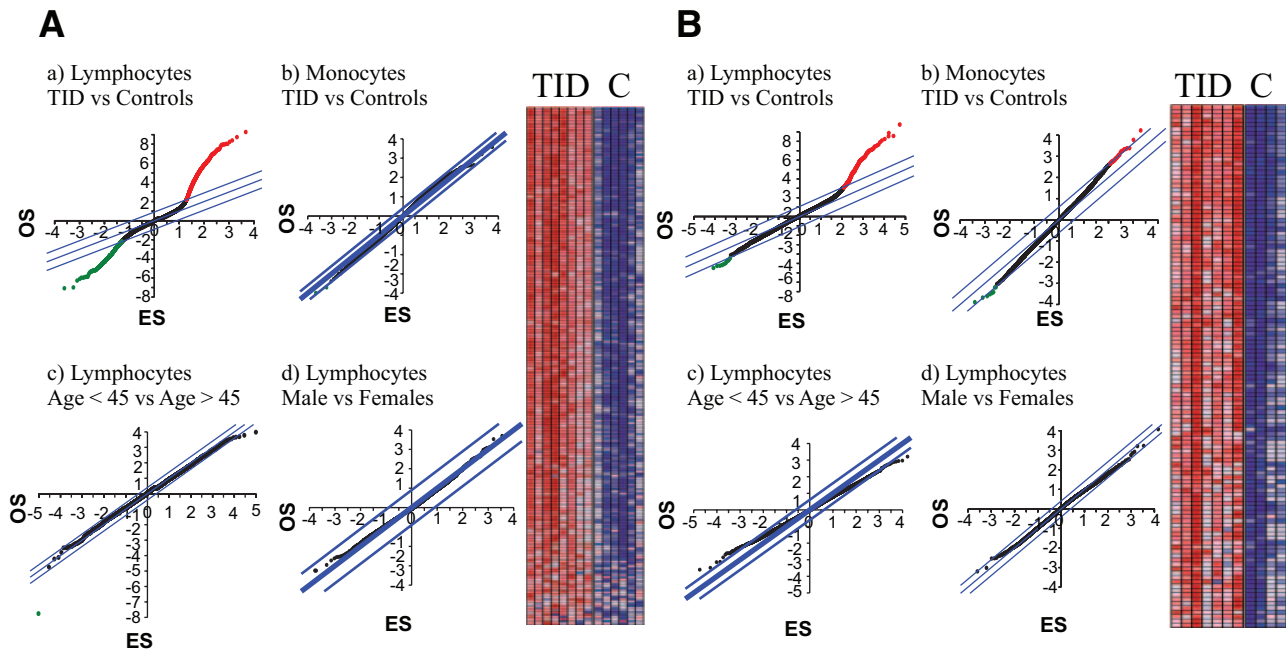
FIG. 2. Analysis of histone H3K9 dimethylation alterations between type 1 diabetic patients (T1D) and healthy control subjects using significance analysis of microarrays (SAM). *A*: Human 12K cDNA array results. *a*: SAM analysis of type 1 diabetic versus healthy control lymphocytes. *b*: Type 1 diabetic versus healthy control monocytes. *c*: Older subjects (age >45) versus younger subjects (age <45). *d*: Men versus women. *Right*: Heatmap of histone H3K9me2 in lymphocytes from type 1 diabetic patients versus healthy control subjects. *B*: Human 12K CpG array results. *a*: SAM analysis of type 1 diabetic versus healthy control lymphocytes. *b*: Type 1 diabetic versus healthy control monocytes. *c*: Older subjects (age >45) versus younger subjects (age <45). *d*: men versus women. *Right panels* in *A* and *B* are heatmaps of H3K9me2 in lymphocytes from type 1 diabetic patients versus healthy control subjects. ES, expected score; OS, observed score. (Please see http://dx.doi.org/10.2337/db08-0645 for a high-quality digital representation of this figure.)

Next, we examined these samples using 12K human CpG island arrays (Fig. 2*B*). Similar to the cDNA array results (Fig. 2*A*), significant increases in H3K9me2 were noted at CpG island regions on a subset of genes in lymphocytes but not monocytes (Fig. 2*B*, *a* and *b*), and these variations were again specific to type 1 diabetes and not dependent on age or sex (Fig. 2*B*, *c* and *d*). Specifically, 213 probes showing increased methylation were identified (heatmap in Fig. 2*B*, *right panel*). The annotation of these "altered" CpG island targets can be summarized as follows: *1*) within promoters, *2*) within gene exons or introns, *3*) within the genome but not close to any genes, and *4*) blank or not found by the BLAST database. Detailed gene information is listed in supplementary Table S2 (available in the online appendix).

Last, we performed ChIP-chips with human promoter tiling arrays using pooled histone H3K9me2 ChIP–enriched samples from eight type 1 diabetic patients or seven healthy control subjects. By using a microarray peak detection program MPeak (27) (details in the supplemental methods in the online appendix), two sets of genes were obtained that displayed H3K9me2 variations between type 1 diabetic patients and healthy control subjects as depicted in the representative heatmap in Fig. 3*A*. The heatmap shows a sample mapping of H3K9me2 enrichment at the first 20 probes in the promoter tiling array. Red areas represent high levels of methylation, whereas blue areas represent no methylation or low levels of methylation. Fig. 3*A*, *left panel*, shows genes depicting higher H3K9me2 in the type 1 diabetic group (hypermethylation), and Fig. 3*A*, *right panel*, is the converse (hypomethylation). We next confirmed that these results obtained by computation analyses are compatible with those displayed by SignalMap, a package provided by Nimblegen for visualizing the promoter tiling array data as shown by

selected hyper- and hypohistone methylation genes in Fig. 3*B*. The complete lists of these two groups of genes are detailed in supplementary Tables S3 and S4, available in the online appendix. Interestingly, *CTLA4*, a known type 1 diabetes susceptibility gene (1), displayed higher H3K9me2 at the promoter region in type 1 diabetic patients. Other interesting methylated genes include *interleukin-1A* (*IL-1A*), *CLCX3*, *tumor necrosis factor* (TNF), *Notch4*, *MAP4K3*, and *RARA* (Fig. 3*B*). It is notable that we recently observed similar H3K9me2 changes at the *IL-1A* promoter in type 1 diabetic patient monocytes and in THP-1 monocyte cells cultured in high glucose.

Collectively, the ChIP-chip profiling with three microarray formats (cDNA, CpG, and promoter tiling arrays) clearly reveals distinct associations between altered histone H3K9me2 and type 1 diabetes (Figs. 2 and 3).

Validation of the H3K9me2 alterations in the microarrays and evaluation of the expression of levels of the corresponding histone K9 methyltransferases in type 1 diabetic patients versus healthy control subjects. To validate the cDNA and CpG array results, 10 probes that displayed increases in H3K9me2 were selected for follow-up conventional ChIP assays with quantitative real-time PCRs (Fig. 4*A*). Nine of the 10 probes showed at least a twofold increase, confirming the accuracy of data generated by our ChIP-chip profiling method.

We next tested whether dysregulated expression of key histone H3K9 methyltransferases or demethylases is responsible for the observed increase in H3K9me2 in the type 1 diabetic patients. G9a is reported to be the primary histone methyltransferase responsible for H3K9me2 (28,29). Quantification of lymphocyte levels of G9a mRNA by quantitative PCR revealed no significant differences between type 1 diabetic patients and healthy control subjects (Fig. 4*B*). In addition, recent studies show there
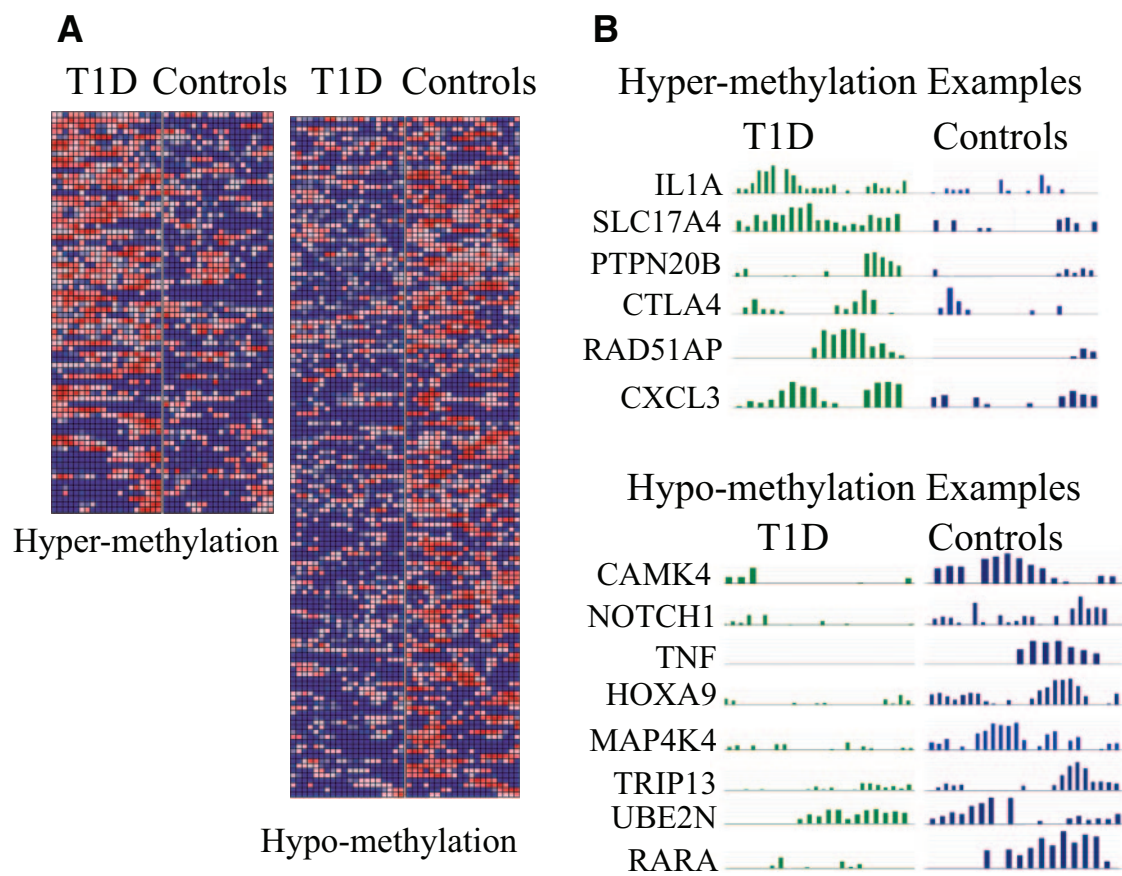
FIG. 3. Promoter tiling array data showing variations of histone H3K9me2 between type 1 diabetic (T1D) patients and healthy control subjects in human promoter regions. *A*: Heatmap of histone H3K9me2 variations in promoter tiling arrays. Histone H3K9me2 ChIPs from type 1 diabetic patients and healthy control subjects (pooled from each group) were hybridized to human promoter tiling arrays (Nimblegen). Using the peak detection program MPeak, we located which promoters on the genome depicted H3K9me2 changes and located their positions by identifying clustered areas of probes that exhibit high ratio values. MPeak results were compiled and filtered for significant peaks with *P* values ≤0.05. A threshold cutoff ratio of twofold was used to generate the set of peaks, and probe-level values were uploaded to GenePattern's HeatMapImage software to create the heatmaps. *B*: Selected examples of hyper- and hypomethylated genes are illustrated by SignalMap. (Please see http://dx.doi.org/10.2337/db08-0645 for a high-quality digital representation of this figure.)

are at least two molecular modules, JMJD1A (30,31) and LSD1 with androgen receptor (30–32), that function as cellular histone H3K9me2 demethylases. Again, we found no significant differences in their expression levels (Fig. 4*B*). These results indicate that the altered histone H3K9me2 patterns observed in type 1 diabetic patients are most likely not caused by differential levels of the related H3K9 methylases or demethylases.

Alteration of histone H3K9me2 at CTLA4 promoter regions reveals an epigenetic role in type 1 diabetes. We next validated the promoter tiling array data. The demonstrated link between *CTLA4* polymorphisms and type 1 diabetes prompted us to further corroborate the association of *CTLA4* with H3K9me2 and other chromatin marks H3K4me3 and H3K4me2. We also analyzed the genes encoding the related molecules *CD28* and *ICOS*, which have costimulatory functions, whereas *CTLA-4* serves as an inhibitory receptor (33). *CD28* and *ICOS* showed very little or no H3K9me2 signals in the tiling array (Fig. 4*C*). All three histone methylation marks were detectable at *CTLA4*, suggesting a complex histone PTM code at the *CTLA4* promoter region, which could be related to its tightly controlled expression pattern in T-cells. Notably, when type 1 diabetic patients and healthy subjects were compared, increased H3K9me2 at the *CTLA4* promoter with reciprocal decreased H3K9me2 at the *ICOS* promoter was noted (Fig. 3*C*, *top*, compare arrows). Furthermore,

by performing follow-up quantitative PCRs with H3K9me2 ChIP–enriched DNA from each individual, we confirmed that this increase in H3K9me2 at the *CTLA4* promoter was statistically significant in type 1 diabetic versus the healthy control groups (Fig. 4*D*, *P* = 0.0023). Because H3K9me2 is considered a repressive mark, the altered H3K9me2 could imply lower *CTLA4* and higher *ICOS* levels in activated T-cells of type 1 diabetes or when they are stimulated. Both scenarios are expected to enhance T-cell activation in type 1 diabetes and are compatible with the key role of dysregulated T-cell activation in type 1 diabetes.

IPA of the gene set showing altered histone H3K9me2 in type 1 diabetes. To evaluate the relevance of the genes displaying increased methylation in cells from type 1 diabetic patients, it is essential to uncover links between these genes and type 1 diabetes. However, as in all microarray studies, it is a daunting task to find biological links between several hundred genes and type 1 diabetes and integrate them within a connected network. Fortunately, powerful bioinformatics tools are now available. We selected the IPA software (www.Ingenuity.com) to further analyze the candidate gene list generated by our ChIP-chips (details in the supplemental methods in the online appendix). Briefly, the list of genes showing increased histone methylation was imported into IPA to construct networks of biological relationships, such as direct physical, pathway, transcriptional, and enzymatic
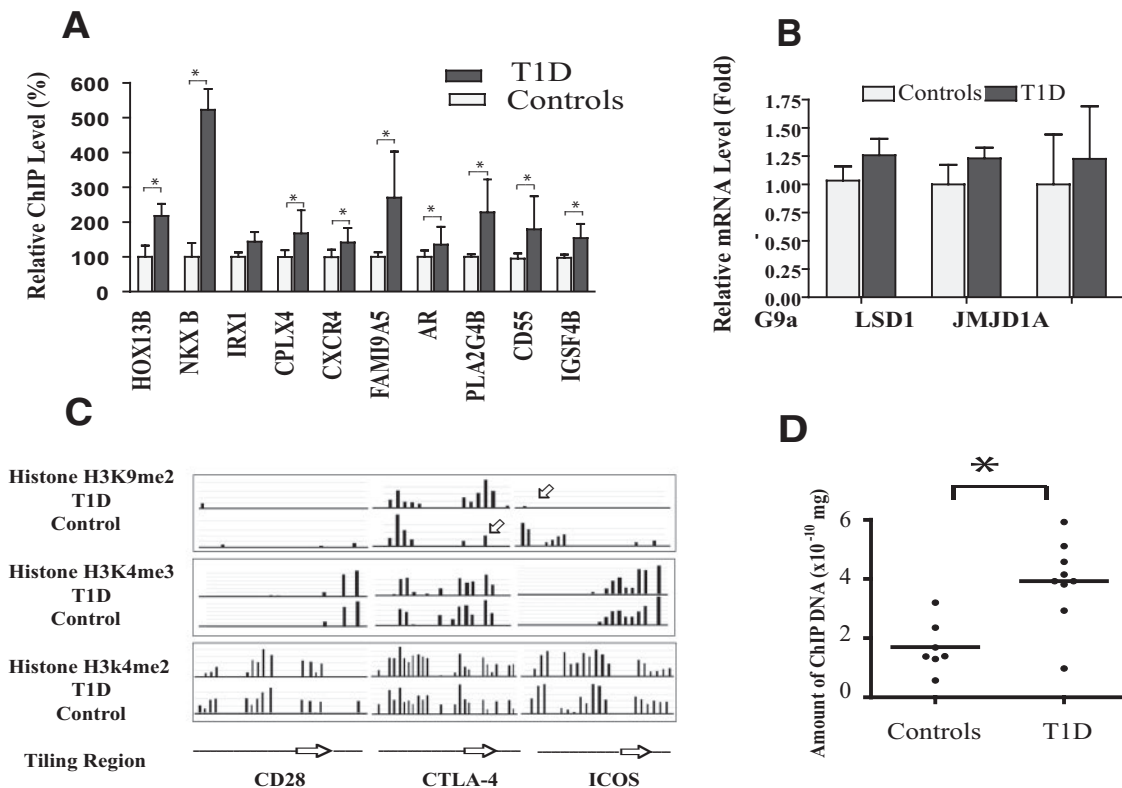
FIG. 4. Validation of histone methylation alterations and quantification of histone methylase/demethylase mRNA levels in type 1 diabetic patients and healthy control subjects. *A*: Validation of histone methylation alterations in cDNA and CpG arrays. Conventional ChIPs were carried out on selected candidate genes to verify the alterations in histone H3K9me2 observed from the ChIP-chip experiments. ChIP real-time quantitative PCR analyses were performed with corresponding primers (listed in the supplemental methods in the online appendix). Results shown are means ± SE of triplet real-time PCRs. *P < 0.05 vs. healthy control subjects, by *t* tests. *B*: Real-time quantitative PCR quantification of histone methylase/demethylase mRNA levels. Total RNAs were prepared from the lymphocytes of six type 1 diabetic patients and six healthy control subjects for mRNA quantification by real-time quantitative PCR. β-Actin was used as internal control. Data shown (mean ± SE) are from two sets of PCRs with each independent patient sample with each sample run in triplicate. *C*: Histone modification status at *CTLA-4*, *CD28*, and *ICOS* promoter regions in lymphocytes from type 1 diabetic patients and healthy control subjects. Pooled histone ChIPs from type 1 diabetic patients and healthy control subjects were hybridized to human promoter tiling arrays, and the data were extracted according to standard operating procedures of NimbleGen. Result was visualized by SignalMap. Arrows indicate hyper- or hypohistone methylation. *D*: Conventional ChIP validation of H3K9me2 modification status at *CTLA4* promoter region in lymphocytes from individual type 1 diabetic patients and the healthy control group. Data show results from typical standardized experiments to quantify the amount of specific modified ChIP DNA in type 1 diabetic patient and healthy control population using real-time quantitative PCR. In this particular experiment, nine type 1 diabetic and seven healthy control samples were included. The results indicate a significantly greater H3K9me2 enrichment at the *CTLA4* promoter region in the type 1 diabetic group relative to healthy control group (*P = 0.0023 vs. healthy control subjects, by *t* tests).

interactions based on published literature. The score of each network computed by IPA indicates the likelihood of the input genes in the network being found together because of random chance.

We first combined gene lists generated from both CpG and cDNA arrays (supplementary Tables S1 and S2) for IPA analysis because all of these genes showed an increase H3K9me2 in type 1 diabetes. Among 307 genes in this list, 162 were mapped to 10 different networks by IPA (listed in supplementary Table S3). The top-scoring network (Fig. 5*A*) with functions in gene expression, organ development, cellular growth, and proliferation had the highest IPA score of 64 compared with the remaining networks. Specifically, this network consisted of 35 interacting nodes (molecules) known to be involved in peroxisome proliferator–activated receptor (PPAR), transforming growth factor-β, nuclear factor-κB (NF-κB), p38 mitogen-activated protein kinase, TLR, IL-6, and Wnt signaling pathways (Fig. 5*A*; Table 1; cDNA and CpG array data) that are associated with inflammatory and autoimmune diseases (34). It is noteworthy that this network is enriched in key transcription factors, such as JUNB, CREBBP, HOXD13, E2F1, ATF1, ELK3, and AR, and also signaling kinases, such as MRK10, MAP3K7, and IRAK1.

Many of these have connections with immune and inflammatory responses and NF-κB activation as seen under diabetic conditions. E2F1 is recently identified as an NF-κB–mediated transcriptional activator (35). In addition, INS and IDE, known candidate genes for type 1 and type 2 diabetes (1,36), are also present in this list.

Next, we used IPA to analyze the methylated genes from the promoter tiling array (supplementary Tables S3 and S4). A total of 214 genes were mapped to eight networks (Table S5), and the highest scoring network with a score of 39 (Fig. 5*B*) is linked to immune response function (Table S5). Most importantly, the major pathways involved in this network also included PPAR, IL-10, NF-κB, and IL-6 signaling pathways (Table 1, promoter array data), which are comparable with the results from the cDNA and CpG array data. Together, the IPA bioinformatics approach demonstrates that genes methylated in type 1 diabetes are enriched in signaling and transcription factors. This suggests that a concerted and synergistic alteration of histone methylation within the identified networks can lead to a coordinated perturbation of above-mentioned pathways in lymphocytes and possibly affect the development of type 1 diabetes and its complications.
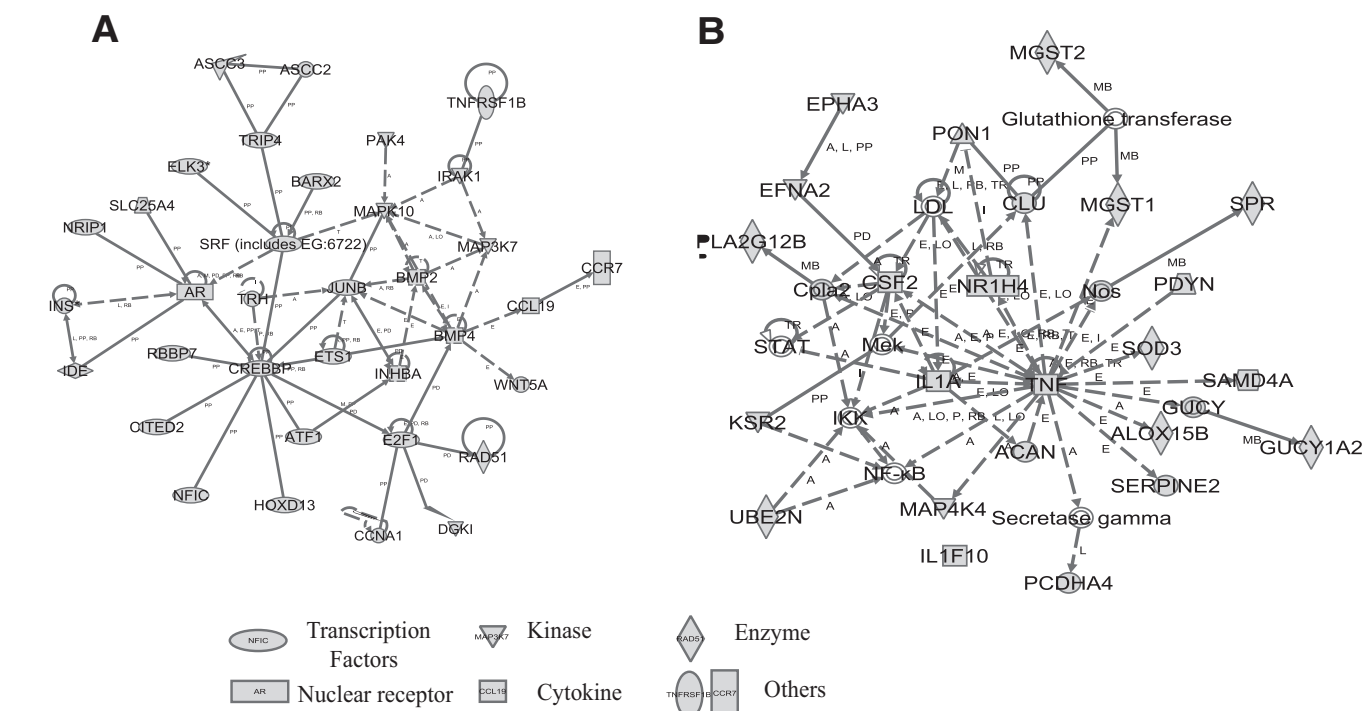
FIG. 5. The networks of altered histone methylation genes created by IPA. The hypothetical networks generated by IPA based on the molecular relationships, interactions, and pathway associations between the methylated candidate genes are shown in a graphical representation. *A*: The top-scoring network consists of 35 focus genes generated from cDNA and CpG arrays data. *B*: The top-scoring network consists of 20 focus genes generated from promoter tiling array data. Proteins are represented as nodes, and the biological relationship between two nodes is represented as an edge (line), which includes interactions, activation, inhibition, proteolysis, phosphorylation, and transcription events. Continuous lines, direct interaction; dotted lines, indirect interaction. A, activation/deactivation; RB, regulation of binding; PP, protein-protein binding; PD, protein-DNA binding; I, inhibition; L, proteolysis; P, phosphorylation/dephosphorylation; T, transcription.

Connections between histone methylation–altered genes and type 1 diabetes candidate genes.

To explore potential relationships of our networks to known type 1 diabetes genes, we took advantage of the IPA database, which has a collection of 62 type 1 diabetes–related genes from previous documented research, including traditional genetic studies (supplementary Table S8, available in the online appendix). We used the pathway explorer feature in IPA, which allowed us to query reported biological relationships between a network and a set of genes based on peer-reviewed publications. As such, we explored the biological relationship or connections between type 1

TABLE 1
Implicated canonical pathways affected by altered histone H3K9me2

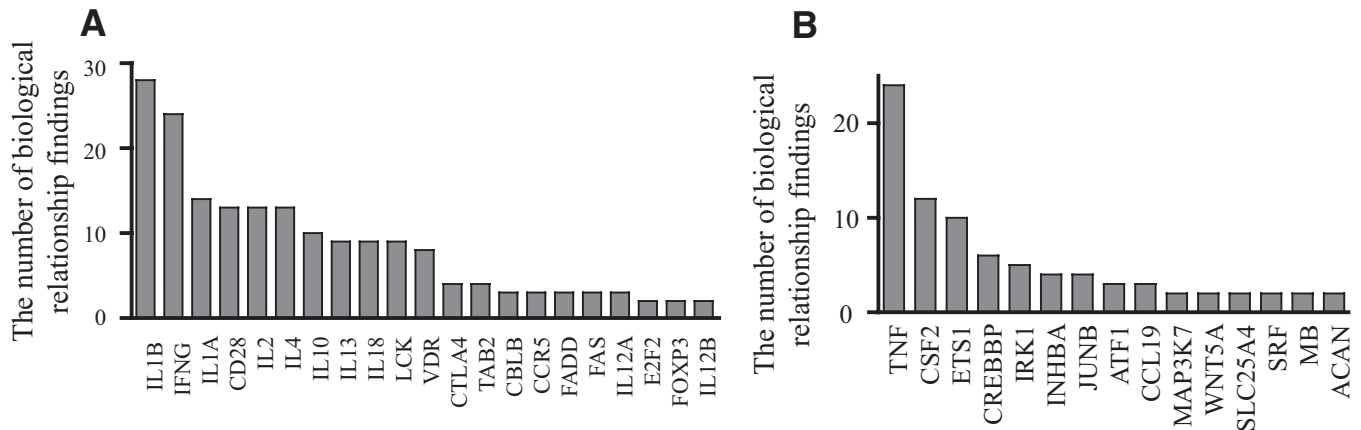| Pathway	Ratio	Molecules
cDNA and CpG array		
PPAR signaling	9.23E-02	CREBBP, INS, CITED2, NRIP1, TNFRSF1B, MAP3K7
Transforming growth factor-β signaling	8.20E-02	CREBBP, INHBA, BMP2, BMP4, MAP3K7
NF-κB signaling	5.45E-02	CREBBP, INS, IRAK1, BMP2, BMP4, MAP3K7
p38 mitogen-activated protein kinase (MAPK) signaling	4.76E-02	ATF1, TNFRSF1B, MAP3K7
TLR signaling	4.35E-02	IRAK1, MAP3K7
IL-6 signaling	4.35E-02	TNFRSF1B, MAPK10, MAP3K7
SAPK/JNK signaling	2.74E-02	MAPK10, MAP3K7
WNT/β-cat signaling	2.21E-02	CREBBP, WNT5A, MAP3K7
Promoter tiling array		
FXR/RXR activation	6.25E-02	PON1, IL1A, NR1H4, RARA, IL1F10, TNF
PPAR signaling	5.26E-02	SRA1, IL1A, MAP4K4, IL1F10, TNF
Glutamate receptor signaling	5.97E-02	GRIN2A, CAMK4, SLC17A6, GRIK2
IL-10 signaling	5.88E-02	IL1A, MAP4K4, IL1F10, TNF
Hepatic cholestasis	3.09E-02	IL1A, NR1H4, RARA, IL1F10, TNF
IL-6 signaling	4.40E-02	IL1A, MAP4K4, IL1F10, TNF
LPS/IL1 inhibition of RXR function	3.08E-02	MGST1, SLC27A2, NR1H4, RARA, CPT1C, TNF
NF-κB signaling	3.50E-02	IL1A, UBE2N, MAP4K4, IL1F10, TNF
LXR/RXR activation	3.70E-02	IL1A, IL1F10, TNF
Xenobiotic metabolism signaling	2.40E-02	AHRR, MGST1, SRA1, IL1A, CAMK4, TNF
p38 MAPK signaling	3.16E-02	IL1A, IL1F10, TNF
Death receptor signaling	3.28E-02	MAP4K4, TNF

FIG. 6. Biological relationships between type 1 diabetes–related genes and our top-scoring networks based on literature findings. Known type 1 diabetes–related genes (Table S6 in the online appendix) were queried for their biological relationships to the identified top-scoring networks (Fig. 5A and B) from our study. The bar graphs show the number of biological relationships between type 1 diabetes–related genes and genes in our networks based on literature findings. Genes are placed in the order of the number of biological relationships from highest (*left*) to lowest (*right*). A: Relationships between type 1 diabetes–related genes with our genes. B: Relationships between our genes and type 1 diabetes–related genes. All biological relationships can also been seen in supplementary Fig. S1 in the online appendix.

diabetes–related genes collected in the IPA database and our two top-scoring networks from Fig. 5. Pathway explorer revealed as many as 162 biological connections between them (supplementary Fig. S1, available in the online appendix). By the order of the number of literature findings of biological relationships, such as direct interactions, transcription, translocation, activation, inhibition, and binding regulation, 21 genes with known association to type 1 diabetes, including *IL-1B*, *IFN*γ, *CD28*, *IL-2*, *IL-4*, *IL-10*, *IL-13*, *IL-18*, *LCK*, *VDR*, and *TAB2*, were found to have connections with genes from our two top-scoring networks (Fig. 6A). Conversely, 15 genes with altered histone methylation from our study were found to have connections with known type 1 diabetes genes (Fig. 6B). These results suggest that the top-scoring networks (Fig. 5) could influence type 1 diabetes through these known type 1 diabetes genes (Fig. 6) and related pathways (supplementary Fig. S1). This not only reaffirms the role of cytokines and inflammation in type 1 diabetes but also provides new mechanistic and epigenetic insights into the pathology of type 1 diabetes.

DISCUSSION

Human peripheral blood is an easily accessible and noninvasive source of primary human cells that has provided valuable genetic and gene expression information for modern medicine. In the current study, for the first time to our knowledge, we have performed ChIP-chip with primary blood cells to examine the correlations between histone methylation and type 1 diabetes by comparing the genome-wide H3K9me2 profiles in lymphocytes and monocytes from type 1 diabetic patients versus healthy control subjects. We observed that a distinct subset of genes in lymphocytes from type 1 diabetic patients show altered histone methylation and that these genes are relevant to the pathology of type 1 diabetes.

It should be underscored that there are key differences between histone methylation profiling and traditional mRNA profiling. The latter has contributed to most of our knowledge of dysregulated gene expression in human diseases. But the instability of mRNA itself, the inherent complexity of transcription networks, and the imbalanced copy number of transcripts could mask the real identity of a specific gene(s) that contributes to underlying human

diseases. Instead, profiling the unvaried copy number and a semistable chromatin mark, such as histone lysine methylation, could be an alternative that reveals the chromatin and epigenetic status of genes in cells. Our eventual prediction of how cells will respond to environmental stimuli based on their histone methylation patterns will be a key benefit. Such epigenomic information could be critical to unmask the underlying mechanisms and pathways causing type 1 diabetes. Histone methylation has recently been linked to cancers (11,37,38), and our recent studies have suggested the relevance to diabetes (19,39). Furthermore, we recently reported that epigenetic histone methylation could be responsible for metabolic memory and sustained diabetic vascular complications (40). Collectively, these data support the study of histone methylation profiling and epigenomics to provide new insights into the pathology of diabetes.

Key proteins that recognize and bind to H3K9me2, including HP1, Suv39h1, G9a, SETDB1, histone deacetylases, and DNMT1, can play repressive roles in transcription (29,41,42). The variations in histone H3K9me2 at gene promoter and coding regions that we observed in this study are likely due to the recruitment of G9a through an unknown mechanism(s), because G9a is the primary histone methylase responsible for H3K9me2 (29), or through histone exchange during transcription (43). This event might be a regulatory feedback inhibition process triggered by the induction of active transcription of a subset of genes. If so, the increased H3K9me2 in gene coding regions implies a recent history of active transcription and may serve as a restraint for subsequent transcription, because of the repressive role of H3K9me2. Thus, one scenario to explain our results is that genes in the network were actively transcribed under diabetic conditions and this leads to G9a/H3K9me2-mediated feedback repression. One of the consequences would be that the expression of these genes will be impaired in the subsequent activation period when the cell receives stimulation signals. Such mechanisms could be significant contributors to the pathogenesis of type 1 diabetes.

Understanding the complex interactions between genes and the environment remains a significant challenge for diabetes and other common diseases. Type 1 diabetes is an autoimmune disease suggested to result from a combina-

tion of environmental triggers and the increased risk conferred by an unknown number of genetic factors. Several biochemical mechanisms have also been shown to mediate the associated cellular dysfunction. Along with DNA sequences, histone methylation and DNA methylation are integral information encoded in the chromatin and epigenome. The growing appreciation of the association between methylation alterations and human diseases arises from the fact that histone methylations are semistable and heritable in somatic cells despite their dynamic nature and thus could have epigenetic effects. However, the complete biological functions of histone methylation need to be fully decoded to clearly predict how cells decipher histone methylation patterns and how alterations in these patterns can relate to disease states. Although the impact of histone methylation variations on common human diseases has been proposed (44,45), to our knowledge, no single genome-wide study has addressed this issue with cells directly from diabetic patients. The current investigation with patient cells is supported by our recent study with cells cultured in vitro, showing that acute diabetic stimuli, such as high glucose, can perturb histone methylation and, importantly, that key genes showing altered methylation were diabetes-related (19). The patients enrolled in the current study all had longstanding type 1 diabetes. Therefore, the observed methylation variations could be related to either type 1 diabetes or its complications. A recent study reveals that several proinflammatory factors are present in the sera of recent-onset type 1 diabetic patients (46). Thus, future studies could determine whether recent-onset type 1 diabetic patients have similar methylation variations. In addition, while choosing control subjects, careful consideration could be given for matching age, sex, geographical region, and major histocompatibility complex haplotypes. Prediabetic subjects could also be assessed. Overall, although there is no doubt that genomic single nucleotide polymorphisms in multiple key genes play decisive roles in type 1 diabetes (1,2), we believe that alterations in epigenetic marks, such as histone methylation, also play important roles, especially when environmental factors influence disease parameters. Such epigenetic changes might also explain the metabolic memory phenomenon observed in the Epidemiology of Diabetes Interventions Complications trial (8,10) in which type 1 diabetic patients continued to develop complications even after subsequent glycemic control. Finally, although it is too early to conclude that epigenetic factors are the causes or consequences of type 1 diabetes, our ChIP-chip genome-wide profiling provides strong evidence of such connections and reveals an epigenetic role for histone H3K9me2 in the lymphocytes of type 1 diabetic patients.

REFERENCES

1. Davies JL, Kawaguchi Y, Bennett ST, Copeman JB, Cordell HJ, Pritchard LE, Reed PW, Gough SC, Jenkins SC, Palmer SM, Balfour KM, Rowe BR, Farrall M, Barnett AH, Bain SC, Todd JA: A genome-wide search for human type 1 diabetes susceptibility genes. *Nature* 371:130–136, 1994
2. Todd JA, Walker NM, Cooper JD, Smyth DJ, Downes K, Plagnol V, Bailey R, Nejentsev S, Field SF, Payne F, Lowe CE, Szeszko JS, Hafler JP, Zeitels L, Yang JH, Vella A, Nutland S, Stevens HE, Schuilenburg H, Coleman G, Maisuria M, Meadows W, Smink LJ, Healy B, Burren OS, Lam AA, Ovington NR, Allen J, Adlem E, Leung HT, Wallace C, Howson JM, Guja C, Ionescu-Tirgoviste C, Simmonds MJ, Heward JM, Gough SC, Dunger DB, Wicker LS, Clayton DG: Robust associations of four new chromosome regions from genome-wide analyses of type 1 diabetes. *Nat Genet* 39:857–864, 2007
3. An Essay by Dr. John Todd [article online], 2002. Available from http://www.esi-topics.com/diabetes/interviews/DrJohnTodd.html
4. Jirtle RL, Skinner MK: Environmental epigenomics and disease susceptibility. *Nat Rev Genet* 8:253–262, 2007
5. Klug A, Rhodes D, Smith J, Finch JT, Thomas JO: A low resolution structure for the histone core of the nucleosome. *Nature* 287:509–516, 1980
6. Jenuwein T, Allis CD: Translating the histone code. *Science* 293:1074–1080, 2001
7. Strahl BD, Allis CD: The language of covalent histone modifications. *Nature* 403:41–45, 2000
8. EDIC Writing Team: Sustained effect of intensive treatment of type 1 diabetes mellitus on development and progression of diabetic nephropathy: the Epidemiology of Diabetes Interventions and Complications (EDIC) Study. *JAMA* 290:2159–2167, 2003
9. Ihnat MA, Thorpe JE, Ceriello A: Hypothesis: the "metabolic memory", the new challenge of diabetes. *Diabet Med* 24:582–586, 2007
10. EDIC Writing Team: Effect of intensive therapy on the microvascular complications of type 1 diabetes mellitus. *JAMA* 287:2563–2569, 2002
11. Shilatifard A: Chromatin modifications by methylation and ubiquitination: implications in the regulation of gene expression. *Annu Rev Biochem* 75:243–269, 2006
12. Sims RJ III, Nishioka K, Reinberg D: Histone lysine methylation: a signature for chromatin function. *Trends Genet* 19:629–639, 2003
13. Tamaru H, Selker EU: A histone H3 methyltransferase controls DNA methylation in *Neurospora crassa*. *Nature* 414:277–283, 2001
14. Bernstein BE, Kamal M, Lindblad-Toh K, Bekiranov S, Bailey DK, Huebert DJ, McMahon S, Karlsson EK, Kulbokas EJ III, Gingeras TR, Schreiber SL, Lander ES: Genomic maps and comparative analysis of histone modifications in human and mouse. *Cell* 120:169–181, 2005
15. Miao F, Natarajan R: Mapping global histone methylation patterns in the coding regions of human genes. *Mol Cell Biol* 25:4650–4661, 2005
16. Mito Y, Henikoff JG, Henikoff S: Genome-scale profiling of histone H3.3 replacement patterns. *Nat Genet* 37:1090–1097, 2005
17. Schubeler D, MacAlpine DM, Scalzo D, Wirbelauer C, Kooperberg C, van Leeuwen F, Gottschling DE, O'Neill LP, Turner BM, Delrow J, Bell SP, Groudine M: The histone modification pattern of active genes revealed through genome-wide chromatin analysis of a higher eukaryote. *Genes Dev* 18:1263–1271, 2004
18. Ren B, Robert F, Wyrick JJ, Aparicio O, Jennings EG, Simon I, Zeitlinger J, Schreiber J, Hannett N, Kanin E, Volkert TL, Wilson CJ, Bell SP, Young RA: Genome-wide location and function of DNA binding proteins. *Science* 290:2306–2309, 2000
19. Miao F, Wu X, Zhang L, Yuan YC, Riggs AD, Natarajan R: Genome-wide analysis of histone lysine methylation variations caused by diabetic conditions in human monocytes. *J Biol Chem* 282:13854–13863, 2007
20. Miao F, Wu X, Zhang L, Riggs AD, Natarajan R: Histone methylation patterns are cell-type specific in human monocytes and lymphocytes and well maintained at core genes. *J Immunol* 180:2264–2269, 2008
21. R Development Core Team: *R: A Language and Environment for Statistical Computing*. Vienna, R Foundation for Statistical Computing, 2003
22. Yang YH, Paquet A, Dudoit S: *marray: Exploratory analysis for two-color spotted microarray data* [article online], 2007. Available from http://bioconductor.org
23. Ihaka R, Gentleman RR: A language for data analysis and graphics. *J Comput Graph Stat* 5:299–314, 1996
24. Gentleman RC, Carey VJ, Bates DM, Bolstad B, Dettling M, Dudoit S, Ellis B, Gautier L, Ge Y, Gentry J, Hornik K, Hothorn T, Huber W, Iacus S, Irizarry R, Leisch F, Li C, Maechler M, Rossini AJ, Sawitzki G, Smith C, Smyth G, Tierney L, Yang JY, Zhang J: Bioconductor: open software development for computational biology and bioinformatics. *Genome Biol* 5:R80, 2004

25. Ingenuity systems [article online]. Available from www.ingenuity.com/products/pathways_analysis.html. Accessed 20 March 2008

26. Tusher VG, Tibshirani R, Chu G: Significance analysis of microarrays applied to the ionizing radiation response. *Proc Natl Acad Sci U S A* 98:5116–5121, 2001

27. Zheng M, Barrera LO, Ren B, Wu YN: ChIP-chip: data, model, and analysis. *Biometrics* 63:787–796, 2007

28. Tachibana M, Sugimoto K, Fukushima T, Shinkai Y: Set domain-containing protein, G9a, is a novel lysine-preferring mammalian histone methyltransferase with hyperactivity and specific selectivity to lysines 9 and 27 of histone H3. *J Biol Chem* 276:25309–25317, 2001

29. Tachibana M, Sugimoto K, Nozaki M, Ueda J, Ohta T, Ohki M, Fukuda M, Takeda N, Niida H, Kato H, Shinkai Y: G9a histone methyltransferase plays a dominant role in euchromatic histone H3 lysine 9 methylation and is essential for early embryogenesis. *Genes Dev* 16:1779–1791, 2002

30. Yamane K, Toumazou C, Tsukada Y, Erdjument-Bromage H, Tempst P, Wong J, Zhang Y: JHDM2A, a JmjC-containing H3K9 demethylase, facilitates transcription activation by androgen receptor. *Cell* 125:483–495, 2006

31. Wissmann M, Yin N, Muller JM, Greschik H, Fodor BD, Jenuwein T, Vogler C, Schneider R, Gunther T, Buettner R, Metzger E, Schule R: Cooperative demethylation by JMJD2C and LSD1 promotes androgen receptor-dependent gene expression. *Nat Cell Biol* 9:347–353, 2007

32. Metzger E, Wissmann M, Yin N, Muller JM, Schneider R, Peters AH, Gunther T, Buettner R, Schule R: LSD1 demethylates repressive histone marks to promote androgen-receptor-dependent transcription. *Nature* 437:436–439, 2005

33. Carreno BM, Collins M: The B7 family of ligands and its receptors: new pathways for costimulation and inhibition of immune responses. *Annu Rev Immunol* 20:29–53, 2002

34. Goodnow CC: Multistep pathogenesis of autoimmune disease. *Cell* 130:25–35, 2007

35. Lim CA, Yao F, Wong JJ, George J, Xu H, Chiu KP, Sung WK, Lipovich L, Vega VB, Chen J, Shahab A, Zhao XD, Hibberd M, Wei CL, Lim B, Ng HH, Ruan Y, Chin KC: Genome-wide mapping of RELA(p65) binding identifies E2F1 as a transcriptional activator recruited by NF-kappaB upon TLR4 activation. *Mol Cell* 27:622–635, 2007

36. Groves CJ, Wiltshire S, Smedley D, Owen KR, Frayling TM, Walker M, Hitman GA, Levy JC, O'Rahilly S, Menzel S, Hattersley AT, McCarthy MI: Association and haplotype analysis of the insulin-degrading enzyme (IDE) gene, a strong positional and biological candidate for type 2 diabetes susceptibility. *Diabetes* 52:1300–1305, 2003

37. Seligson DB, Horvath S, Shi T, Yu H, Tze S, Grunstein M, Kurdistani SK: Global histone modification patterns predict risk of prostate cancer recurrence. *Nature* 435:1262–1266, 2005

38. Fraga MF, Ballestar E, Villar-Garea A, Boix-Chornet M, Espada J, Schotta G, Bonaldi T, Haydon C, Ropero S, Petrie K, Iyer NG, Perez-Rosado A, Calvo E, Lopez JA, Cano A, Calasanz MJ, Colomer D, Piris MA, Ahn N, Imhof A, Caldas C, Jenuwein T, Esteller M: Loss of acetylation at Lys16 and trimethylation at Lys20 of histone H4 is a common hallmark of human cancer. *Nat Genet* 37:391–400, 2005

39. Miao F, Gonzalo IG, Lanting L, Natarajan R: In vivo chromatin remodeling events leading to inflammatory gene transcription under diabetic conditions. *J Biol Chem* 279:18091–18097, 2004

40. Villeneuve LM, Reddy MA, Lanting LL, Wang M, Meng L, Natarajan R: Epigenetic histone H3 lysine 9 methylation in metabolic memory and inflammatory phenotype of vascular smooth muscle cells in diabetes. *Proc Natl Acad Sci U S A* 105:9047–9052, 2008

41. Rice JC, Briggs SD, Ueberheide B, Barber CM, Shabanowitz J, Hunt DF, Shinkai Y, Allis CD: Histone methyltransferases direct different degrees of methylation to define distinct chromatin domains. *Mol Cell* 12:1591–1598, 2003

42. Peters AH, Kubicek S, Mechtler K, O'Sullivan RJ, Derijck AA, Perez-Burgos L, Kohlmaier A, Opravil S, Tachibana M, Shinkai Y, Martens JH, Jenuwein T: Partitioning and plasticity of repressive histone methylation states in mammalian chromatin. *Mol Cell* 12:1577–1589, 2003

43. Stewart MD, Sommerville J, Wong J: Dynamic regulation of histone modifications in Xenopus oocytes through histone exchange. *Mol Cell Biol* 26:6890–6901, 2006

44. Bjornsson HT, Fallin MD, Feinberg AP: An integrated epigenetic and genetic approach to common human disease. *Trends Genet* 20:350–358, 2004

45. Feinberg AP: Phenotypic plasticity and the epigenetics of human disease. *Nature* 447:433–440, 2007

46. Wang X, Jia S, Geoffrey R, Alemzadeh R, Ghosh S, Hessner MJ: Identification of a molecular signature in human type 1 diabetes mellitus using serum and functional genomics. *J Immunol* 180:1929–1937, 2008